Low energy cost for optimal speed and control of membrane fusion

Claire François-Martin[a,b,c], James E. Rothman[d,e,1], and Frederic Pincet[a,b,c,d,e,1]

[a]Laboratoire de Physique Statistique, Ecole Normale Supérieure, Paris Sciences et Lettres Research University, 75005 Paris, France; [b]Laboratoire de Physique Statistique, Université Paris Diderot Sorbonne Paris Cité, 75005 Paris, France; [c]Laboratoire de Physique Statistique, Sorbonne Universités, Université Pierre et Marie Curie, Univ Paris 06, CNRS, 75005 Paris, France; [d]Department of Cell Biology, School of Medicine, Yale University, New Haven, CT 06520; and [e]Nanobiology Institute, School of Medicine, Yale University, New Haven, CT 06520

Contributed by James E. Rothman, December 28, 2016 (sent for review December 15, 2016; reviewed by Gary Bryant and Ivan Lopez-Montero)

Membrane fusion is the cell's delivery process, enabling its many compartments to receive cargo and machinery for cell growth and intercellular communication. The overall activation energy of the process must be large enough to prevent frequent and nonspecific spontaneous fusion events, yet must be low enough to allow it to be overcome upon demand by specific fusion proteins [such as soluble *N*-ethylmaleimide–sensitive factor attachment protein receptors (SNAREs)]. Remarkably, to the best of our knowledge, the activation energy for spontaneous bilayer fusion has never been measured. Multiple models have been developed and refined to estimate the overall activation energy and its component parts, and they span a very broad range from 20 k_BT to 150 k_BT, depending on the assumptions. In this study, using a bulk lipid-mixing assay at various temperatures, we report that the activation energy of complete membrane fusion is at the lowest range of these theoretical values. Typical lipid vesicles were found to slowly and spontaneously fully fuse with activation energies of ∼30 k_BT. Our data demonstrate that the merging of membranes is not nearly as energy consuming as anticipated by many models and is ideally positioned to minimize spontaneous fusion while enabling rapid, SNARE-dependent fusion upon demand.

membrane fusion | activation energy | liposome | energy landscape | lipid-mixing assay

Living organisms and cells are composed of different compartments delimited by a membrane. These compartments have their own function and integrity but nevertheless need to communicate with one another. A common pathway by which exchanges can occur between them is membrane fusion, a crucial process leading to the opening of a fusion pore connecting two compartments and allowing their respective contents to mix or react (1, 2). The global effective activation energy of the process must be large enough to avoid frequent spontaneous membrane fusion events. Nevertheless, it must remain sufficiently low so that proteins like soluble *N*-ethylmaleimide–sensitive factor attachment protein receptors (SNAREs) (3–5) are able to overcome it and induce fusion. If multiple models (6–16) have been developed and refined to estimate this activation energy, there is still a lack of experimental data to provide its actual value and validate these models. Activation energies have been reported between intermediate states of the fusion process (17) or with nonphospholipid surfactants (18). They were obtained with nonspontaneous fusion triggered by an external source such as osmotic pressure or mechanical shear.

Here, by using a minimal membrane model system, we show that the activation energy of complete and spontaneous membrane fusion is in the lowest range of the predicted values. Lipid vesicles composed of 1-palmitoyl-2-oleoyl-*sn*-glycero-3-phosphocholine (POPC) or 1,2-dioleoyl-*sn*-glycero-3-phosphocholine (DOPC) were found to slowly and spontaneously fully fuse with respective activation energies of 26.4 ± 1 k_BT and 34.3 ± 0.8 k_BT. Our data demonstrate that the merging of membranes is not as energy consuming as anticipated in the early models.

Whereas key aspects of the transition states remain unclear, lipid bilayer fusion likely involves intermediates (19) and is therefore kinetically complex. With this in mind, we take a more global view, in which kinetic complexity and molecular rearrangements are averaged to enable a simple experimental approach to measure activation energy by population analysis. Working in bulk with small phospholipid vesicles that undergo random Brownian motion provides an ideally controlled minimal system to monitor fusion on a large scale. Vesicles collide and, on very rare occasions, these collisions are sufficiently energy yielding to trigger fusion. When fusion is intentionally triggered by proteins like SNAREs or physicochemical factors such as osmotic pressure, conditions are invariably chosen to minimize the rate of this spontaneous fusion so the fusion signal resulting from these rare spontaneous events is negligible (3, 20). In principle, at high collision frequency, these fusion events can become numerous enough to be observable. Hence, to observe and quantify spontaneous fusion, we chose to use a classical bulk fusion assay with increased collision rate by working at high vesicle concentration with refined analysis.

Fusion among ∼60-nm diameter phosphatidylcholine (PC) vesicles at 37 °C was monitored using a well-established lipid-mixing assay (21) (*SI Methods*). Briefly, two sets of vesicles were mixed together. One set of vesicles contained two types of fluorescent lipids tagged with either 7-nitro-2-1,3-benzoxadiazol-4-yl (NBD) or lissamine rhodamine B (Rh). These fluorescent lipids were present at concentrations at which NBD is largely quenched by Rh through Förster resonance energy transfer (FRET). The other set of vesicles was not fluorescent. When a fusion event occurs between a fluorescent vesicle and a nonfluorescent vesicle,

Significance

Membrane fusion is a key process for cell growth and intercellular communication. There are many models for fusion with widely divergent activation energies. Surprisingly, no comprehensive quantification of fusion was ever experimentally performed. Probably this is because of the difficulty of observing and quantifying rare spontaneous fusion events and equally the difficulty of establishing that such events are *bona fide* fusion events. Here, we find that the activation energy is lower by far than in most predictions. The biological importance of this low energy value is that it explains how cells can maintain traffic among distinct compartments without mixing them up, preventing spontaneous fusion but allowing specific delivery of cargo as soon as fusion-inducing proteins are in place.

Author contributions: C.F.-M., J.E.R., and F.P. designed research; C.F.-M. performed research; C.F.-M., J.E.R., and F.P. analyzed data; and C.F.-M., J.E.R., and F.P. wrote the paper.

Reviewers: G.B., RMIT University; and I.L.-M., Universidad Complutense de Madrid.

The authors declare no conflict of interest.

[1]To whom correspondence may be addressed. Email: pincet@lps.ens.fr or james.rothman@yale.edu.

This article contains supporting information online at www.pnas.org/lookup/suppl/doi:10.1073/pnas.1621309114/-/DCSupplemental.

the mixing of their lipids leads to dilution of the dyes in the resulting combined membrane. This dilution is associated with a decrease of FRET and can be experimentally observed as an increase in NBD fluorescence that, when monitored in bulk, directly yields the number of fusion events per second, i.e., fusion speed (3). To optimize the collision rate, vesicles were incubated at unusually high concentrations (18 mM PC). The results presented in Fig. 1*A* show that lipid mixing was indeed readily observed, suggesting that detectable fusion-like events were occurring in the vesicle solution on experimental timescales (~1 h).

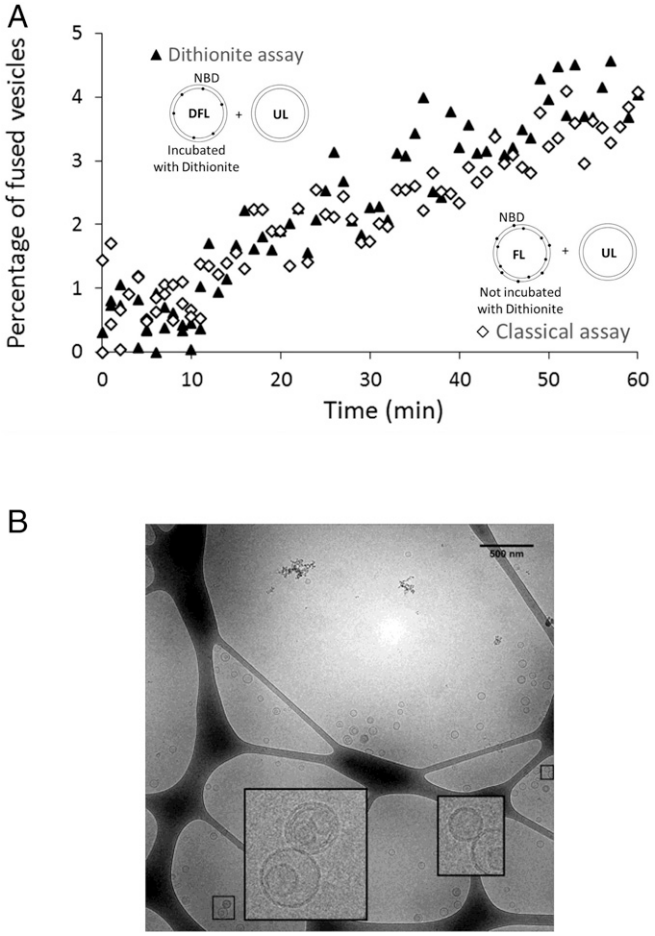

Fig. 1. Full fusion is achieved spontaneously in a suspension of POPC vesicles and intermediate states are transient. (*A*) In the classical lipid-mixing assay (open diamonds), where the fusion of fluorescent and nonfluorescent vesicles is monitored (main text and *SI Methods*), the increase of the fluorescence intensity of NBD shows that lipid mixing takes place and, hence, suggests that fusion-like events occur. The dithionite assay (open triangles), monitoring the fusion of fluorescent vesicles pretreated with dithionite and nonfluorescent vesicles, shows that mixing of lipids coming from the inner leaflets occurs. The dithionite pretreatment of the fluorescent vesicles removes NBD (solid circles in the schematic vesicles) from the outer leaflets of vesicles. Rh is present on both leaflets and is not represented on the schematic vesicles. This demonstrates that full-fusion events occur. The perfect superimposition of both curves (diamonds and triangles) proves that neither hemifusion nor lipid exchange through the solvent significantly occurs and that the large majority of the events leading to lipid mixing are full fusion. (*B*) Representative cryo-EM micrograph. The enlarged pairs of vesicles represent two of the rare cases in which two vesicles are in close apposition. The presence of vesicles inside the largest one (which was observed in the minority of the vesicles) only lowered the effective concentration of vesicles. Because we always used the same pool of vesicles for all temperatures, this does not affect the results. (Scale bar, 500 nm.) No hemifusion diaphragm was observed among 4,215 vesicles, which would correspond to ~150 fusion events (*SI Methods*). The size distribution of the vesicles was determined using similar cryo-EM micrographs (Fig. S2).

Before quantifying the energies involved, the remaining difficulty was to determine what these events actually correspond to: Are they full fusion, intermediate fusion states, or merely lipid exchange without fusion? To discriminate among these possibilities, we monitored lipid mixing of the inner leaflets only. The fluorescent-lipid–containing vesicles were first preincubated with dithionite (*SI Methods*), which quenches NBD's fluorescence as it chemically reduces the NBD groups on the external leaflet only because dithionite does not cross lipid bilayers (22). Because the resulting vesicles had only fluorescent NBD in their inner leaflets (Fig. S1), any FRET changes resulting from incubation with the unlabeled vesicles could only be due to a dilution of their inner leaflet lipids, i.e., full fusion events, and not hemifusion (mixing of outer leaflets without inner leaflet fusion) or exchange of lipids between vesicles via their outer leaflets. Inner leaflet mixing was indeed observed at essentially the same rate as total lipid mixing (Fig. 1*A*), implying that the vast majority of the FRET signal was due to full fusion. To independently confirm this conclusion, we observed the samples by cryo-electron microscopy following incubation (60 min at 37 °C). Stable, extended hemifusion structures are readily observable by this method (23). However, we observed no such hemifusion diaphragms among the 4,215 vesicles. Because FRET experiments show that ~2% of the vesicles have fused at the end of the experiment at 37 °C (or 4% have hemifused), ~150 hemifusion diaphragms could have potentially been observed. This result suggests that at least ~99% of the events led to full fusion (Fig. 1*B* and *SI Text*). Taken together, the dithionite and cryo-EM results show that full vesicle fusion can result solely from spontaneous collisions in the course of Brownian motion and that, on the timescale of our experiment, i.e., minutes, vesicles either remained intact or underwent complete fusion.

Thus, the process of spontaneous fusion among a large population of vesicles can be formulated as a two-state kinetic transition from two separate vesicles to a single vesicle because the lifespan of the intermediate states must be much shorter than the timescale of the experiment. This in turn establishes from a physical viewpoint that spontaneous fusion of vesicles represents a system to which Kramer's theory of reaction rates applies (24, 25). In the overdamped limit of this theory, the transition rate, which here is the speed of spontaneous fusion, follows a simple Arrhenius-like expression: $v = v_0 \exp(-E_a/k_BT)$, where k_B is the Boltzmann constant, v_0 is the frequency factor that depends on many parameters including the collision rate and the density of defects on the membrane, and E_a is an effective activation energy. The energy of the fusion process can thus be reduced to a single activation energy that corresponds to the height of the one energy barrier that must be overcome for full fusion to proceed and would be crossed with the same probability as the actual, much more complex, energy landscape of the entire process. Because the Arrhenius law stipulates that the speed of spontaneous fusion increases with temperature in an E_a-dependent manner, we studied the fusion of POPC (16:0-18:1 PC) and DOPC [18:1 (Δ9-Cis) PC] vesicles at temperatures ranging from 27 °C to 47 °C (Fig. 2*A*) to determine their activation energies for fusion at 37 °C, the physiological temperature. Because E_a and v_0 may vary with the temperature in a logarithmic way compared with $\exp(-E_a/k_BT)$ (24–26), we chose a range of temperature that is small enough to remain close to 37 °C and large enough to observe clear variations of the fusion speed. Over this temperature range, the results showed that variations in the fusion speed are sufficiently large to accurately determine E_a at 37 °C. The initial speeds of fusion were deduced from the initial slopes of the fusion curves (*SI Text*). For both POPC and DOPC, the initial fusion speed varies with 1/T in an exponential manner, which a posteriori validates the Arrhenius-like dependence of

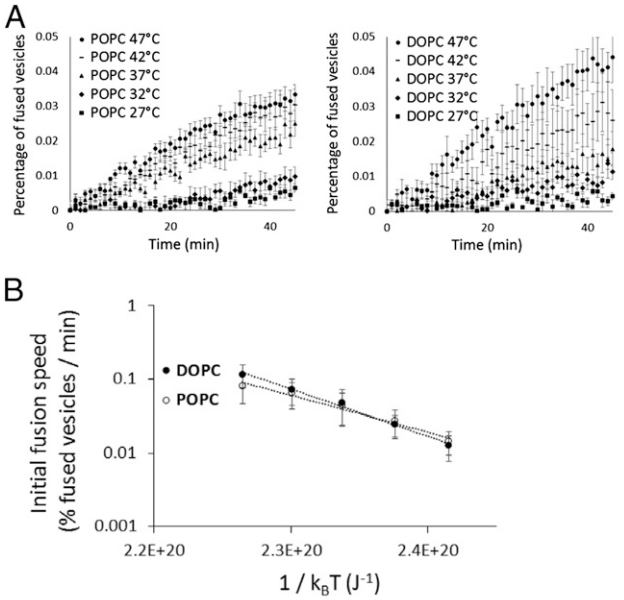

C

Lipid composition	Fit (average data)	E_a (average data)	E_a
POPC	$y = 1.36E+08e^{-1.14E-19x}$	26.6 k_BT	26.4 ± 1.0 k_BT
DOPC	$y = 3,27E+11e^{-1,47E-19x}$	34.3 k_BT	34.3 ± 0.8 k_BT

Fig. 2. Estimate of the activation energy of POPC and DOPC vesicles fusion. (*A*) Fusion assays are performed at different temperatures (27–47 °C). The averages of six independent experiments are represented. The initial time ($t = 0$) is the time when the temperature was stabilized. The speed of fusion increases with temperature. Error bars are SEs on the mean. (*B*) Initial spontaneous fusion speeds are represented vs. the temperature (average of nine independent experiments for POPC and four for DOPC, error bars being SDs) and fitted by exponentials. Speeds of fusion were determined due to the initial slope of the curve representing the percentage of fused vesicles per minute (*SI Text*). (*C*) The exponential fits allow the determination of the activation energies for both reactions, here fusion. Independent fits were also performed for the different experiments, hence allowing the estimation of the error on the measurement (SE on the mean): 26.4 ± 1 k_BT for POPC and 34.3 ± 0.8 k_BT for DOPC.

the fusion speed (Fig. 2*B*). The activation energy values were determined through independent fits of the different experiments (nine for POPC and four for DOPC): 26.4 ± 1.0 k_BT for POPC and 34.3 ± 0.8 k_BT for DOPC at 37 °C (Fig. 2*C*, error bars are SE on the mean). To ensure that these values were not affected by the rate of collision of the liposomes we performed the same measurements at lower concentrations, 6 mM and 12 mM, without any change in the resulting activation energies.

For a more complex reaction pathway to result in the same overall probability of transition to the fused state as a pathway with a single activation barrier, the E_a deduced from the Arrhenius law in the simple two-state model must be larger than, or close to, any of the individual energy barriers that separate successive transient intermediate states in the more complex reaction process, as illustrated in Fig. 3. Because most published models of the fusion process have focused on these proposed individual energy barriers, our results now make it possible to objectively evaluate the plausibility of these models. For both DOPC and POPC, we measured E_a close to 30 k_BT. Such a low value for the overall fusion process was never predicted but remains consistent with recently published coarse-grained simulations (14, 16) in which there is no prior hypothesis concerning the fusion pathway, thereby allowing the predicted transition structures and activation energies to emerge directly. Our measured global E_a is indeed larger than or close to these. According to Smirnova et al. (14), 20 k_BT are required for stalk formation whereas Ryham et al. (16) evaluated activation energies of 31 k_BT (stalk) and 35 k_BT (fusion pore). Thus, these predictions are compatible with our experimental measurements and may closely reproduce the reality of the fusion process at a molecular scale. The previous theoretical studies predicted E_a much larger than 30 k_BT, ranging from 43 k_BT to 170 k_BT (10). Therefore, the assumptions underlying these models seem unlikely to hold.

An activation energy of ∼30 k_BT can also be related to the short-range interactions between membranes that were characterized in the 1980s by Rand and Parsegian (27, 28). Using osmotic pressure, they compressed lamellar phases while measuring their interbilayer separation distance (d). They found that the pressure decreased exponentially with d for all phospholipids: $P(d) = P_0 \exp(-d/\lambda)$. This pressure results from the need to remove the bound water from the polar heads of the lipids as the distance shortens and/or from the entropic repulsion of the headgroups. The prefactor P_0 and the decay (nonspecific) length λ depended on the lipid composition but remained within the same range, 10^9 Pa and 0.15 nm, respectively. Rand and Parsegian also observed that the lamellar phases were usually unstable when the distance was below ∼1 nm, at which point an all-or-none transition to a nonlamellar phase occurred, which these authors suggested resembles the transition from unfused to fused states for vesicles. With these values, the surface energy required for the transition is of the order of 1 mJ/m^2 (*SI Text*). The 30 k_BT would be distributed over an area of ∼600 nm^2 (*SI Text*) and therefore involve only ∼1,000 phospholipids [which occupy about 0.7 nm^2 surface each (27)]. Although the analogy between the two systems is clearly imperfect because there are many subtle uncontrolled aspects such as kinetics and membrane tension, this value would correspond to the cooperative unit of surface on which the future fusion pore will develop and is compatible. This size seems reasonable because it is compatible with the radius of the initial fusion pore, which is thought to be close to 1 nm (29).

Finally, 30 k_BT is an ideal value to enable facile membrane fusion as directed on demand in living cells: It will not happen spontaneously between bare membranes, yet as soon as specific fusion machinery is in place, it will be easily triggered. Fusion between two given membranes is a stochastic event that occurs on average after a time $\tau = \tau_0 \exp(E_a/k_BT)$. Depending on the context (membranes, geometry), the prefactor is between 10^{-10} s and 10^{-6} s (24, 30). For $E_a = 30\ k_BT$, spontaneous fusion will occur between closely apposed phospholipid membranes after

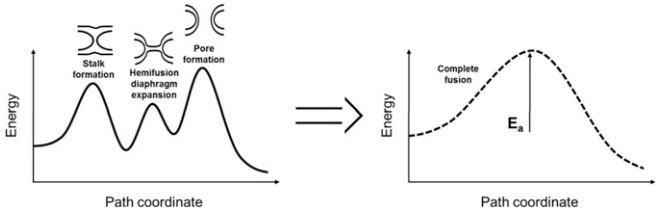

Fig. 3. Lipid bilayer fusion's energy landscapes of decreasing complexity. (*Left*) Schematics of a typical model of the complete energy landscape of the fusion pathway of lipid bilayers. It exhibits three energy barriers: one for the stalk formation, one for the expansion of the hemifusion diaphragm, and one for the opening of the fusion pore. (*Right*) Schematics of an effective energy landscape of the fusion pathway. The three former energy barriers can be represented by one effective energy barrier, of which the height corresponds to the effective activation energy (E_a) of the overall process of fusion. The speed of fusion then follows Arrhenius's law, $v = v_0 \exp(-E_a/k_BT)$, and is the same for the three-barrier and one-barrier fusion pathways.

15 min to 100 d (*SI Text*). Therefore, at the relevant biological scale at which specific fusion occurs (seconds to minutes) it will very seldom happen. However, a single SNAREpin in place between the membranes will significantly lower the activation energy barrier and allow fusion to proceed on the biological timescale. For example, even assuming that the assembly of the linker domain in the C-terminal region of the cytosolic portion is the sole energy supplier for bilayer fusion, the reduction in activation energy will be $\sim 10\ k_BT$ (31), so E_a now becomes $\sim 20\ k_BT$, which lowers the average time for fusion to the range 50 ms to 5 min, depending on the prefactor. This result explains why a single SNARE complex can mediate many fusion processes in isolated systems (32, 33). When more SNARE complexes are involved, the activation energy is correspondingly reduced and the time required becomes exponentially shorter. This increase in the number of SNARE complexes is necessary in specific cases such as neurotransmission in which synaptic vesicles must fuse with the presynaptic plasma membrane in less than 1 ms (34). This drastic timescale change shows that our measured value for activation energy of $\sim 30\ k_BT$ is an elegant balance that nature has made, preventing spontaneous fusion, thus allowing the cell to maintain distinct membrane-bound compartments, yet quickly overcoming this barrier when SNARE and other fusion-inducing proteins are put in place, thus enabling specific traffic among these compartments.

ACKNOWLEDGMENTS. The authors are grateful to Dr. Abdou-Rachid Thiam for fruitful discussions and Dr. Steve Donaldson for reading and commenting on the manuscript. The authors thank Aurélie Di Cicco for the Cryo-EM experiments that were supported by the French National Research Agency through the "Investments for the Future" program [France-BioImaging, Agence Nationale de la Recherche (ANR) Grant ANR-10-INSB-04] and were performed at the Plateforme Imagerie Cellulaire et Tissulaire of the Institut Curie, Paris, member of the France-BioImaging national research infrastructure. C.F.-M. thanks the Direction Générale de l'Armement for financial support. This work was supported by Grant ANR-14-1CHN-0022-01 (to J.E.R.).

1. Jahn R, Lang T, Südhof TC (2003) Membrane fusion. *Cell* 112(4):519–533.
2. Rothman JE (2014) The principle of membrane fusion in the cell (Nobel lecture). *Angew Chem Int Ed Engl* 53(47):12676–12694.
3. Weber T, et al. (1998) SNAREpins: Minimal machinery for membrane fusion. *Cell* 92(6): 759–772.
4. Jahn R, Scheller RH (2006) SNAREs–engines for membrane fusion. *Nat Rev Mol Cell Biol* 7(9):631–643.
5. Wickner W, Schekman R (2008) Membrane fusion. *Nat Struct Mol Biol* 15(7):658–664.
6. Kozlov MM, Leikin SL, Chernomordik LV, Markin VS, Chizmadzhev YA (1989) Stalk mechanism of vesicle fusion. Intermixing of aqueous contents. *Eur Biophys J* 17(3):121–129.
7. Siegel DP (1993) Energetics of intermediates in membrane fusion: Comparison of stalk and inverted micellar intermediate mechanisms. *Biophys J* 65(5):2124–2140.
8. Kuzmin PI, Zimmerberg J, Chizmadzhev YA, Cohen FS (2001) A quantitative model for membrane fusion based on low-energy intermediates. *Proc Natl Acad Sci USA* 98(13): 7235–7240.
9. Markin VS, Albanesi JP (2002) Membrane fusion: Stalk model revisited. *Biophys J* 82(2):693–712.
10. Kozlovsky Y, Kozlov MM (2002) Stalk model of membrane fusion: Solution of energy crisis. *Biophys J* 82(2):882–895.
11. Kozlovsky Y, Chernomordik LV, Kozlov MM (2002) Lipid intermediates in membrane fusion: Formation, structure, and decay of hemifusion diaphragm. *Biophys J* 83(5): 2634–2651.
12. May S (2002) Structure and energy of fusion stalks: The role of membrane edges. *Biophys J* 83(6):2969–2980.
13. Kozlovsky Y, Efrat A, Siegel DP, Kozlov MM (2004) Stalk phase formation: Effects of dehydration and saddle splay modulus. *Biophys J* 87(4):2508–2521.
14. Smirnova YG, Marrink SJ, Lipowsky R, Knecht V (2010) Solvent-exposed tails as prestalk transition states for membrane fusion at low hydration. *J Am Chem Soc* 132(19): 6710–6718.
15. Kawamoto S, Shinoda W (2014) Free energy analysis along the stalk mechanism of membrane fusion. *Soft Matter* 10(17):3048–3054.
16. Ryham RJ, Klotz TS, Yao L, Cohen FS (2016) Calculating transition energy barriers and characterizing activation states for steps of fusion. *Biophys J* 110(5):1110–1124.
17. Lee J, Lentz BR (1998) Secretory and viral fusion may share mechanistic events with fusion between curved lipid bilayers. *Proc Natl Acad Sci USA* 95(16):9274–9279.
18. Porcar L, Hamilton WA, Butler PD, Warr GG (2004) Topological relaxation of a shear-induced lamellar phase to sponge equilibrium and the energetics of membrane fusion. *Phys Rev Lett* 93(19):198301.
19. Chernomordik LV, Kozlov MM (2008) Mechanics of membrane fusion. *Nat Struct Mol Biol* 15(7):675–683.
20. Meyenberg K, Lygina AS, van den Bogaart G, Jahn R, Diederichsen U (2011) SNARE derived peptide mimic inducing membrane fusion. *Chem Commun* 47(33):9405–9407.
21. Struck DK, Hoekstra D, Pagano RE (1981) Use of resonance energy transfer to monitor membrane fusion. *Biochemistry* 20(14):4093–4099.
22. McIntyre JC, Sleight RG (1991) Fluorescence assay for phospholipid membrane asymmetry. *Biochemistry* 30(51):11819–11827.
23. Hernandez JM, et al. (2012) Membrane fusion intermediates via directional and full assembly of the SNARE complex. *Science* 336(6088):1581–1584.
24. Kramers HA (1940) Brownian motion in a field of force and the diffusion model of chemical reactions. *Physica* 7:284–304.
25. Hanggi P, Talkner P, Borkovec M (1990) Reaction-rate theory - 50 years after Kramers. *Rev Mod Phys* 62(2):251–341.
26. Evans E, Smith BA (2011) Kinetics of hole nucleation in biomembrane rupture. *New J Phys* 13:095010.
27. Rand RP, Parsegian VA (1989) Hydration forces between phospholipid-bilayers. *Biochim Biophys Acta* 988(3):351–376.
28. Rand RP, Parsegian VA (1986) Mimicry and mechanism in phospholipid models of membrane fusion. *Annu Rev Physiol* 48:201–212.
29. Breckenridge LJ, Almers W (1987) Currents through the fusion pore that forms during exocytosis of a secretory vesicle. *Nature* 328(6133):814–817.
30. Evans E (2001) Probing the relation between force–lifetime–and chemistry in single molecular bonds. *Annu Rev Biophys Biomol Struct* 30:105–128.
31. Zorman S, et al. (2014) Common intermediates and kinetics, but different energetics, in the assembly of SNARE proteins. *eLife* 3:e03348.
32. Shi L, et al. (2012) SNARE proteins: One to fuse and three to keep the nascent fusion pore open. *Science* 335(6074):1355–1359.
33. van den Bogaart G, et al. (2010) One SNARE complex is sufficient for membrane fusion. *Nat Struct Mol Biol* 17(3):358–364.
34. Sudhof TC (2004) The synaptic vesicle cycle. *Annu Rev Neurosci* 27:509–547.
35. Evans E (1991) Entropy-driven tension in vesicle membranes and unbinding of adherent vesicles. *Langmuir* 7(9):1900–1908.
36. Parlati F, et al. (1999) Rapid and efficient fusion of phospholipid vesicles by the alpha-helical core of a SNARE complex in the absence of an N-terminal regulatory domain. *Proc Natl Acad Sci USA* 96(22):12565–12570.